

LOW CYCLE FATIGUE AND CYCLIC PLASTICITY BEHAVIOR OF INDIAN PHWR / AHWR PRIMARY PIPING MATERIAL

Sumit Goyal^{1*}, S. K. Gupta¹, S. Sivaprasad², S. Tarafder², V. Bhasin¹, K. K. Vaze¹, A. K. Ghosh³

¹Bhabha Atomic Research Centre, Mumbai 400085, India

²National Metallurgical Laboratory, Jamshedpur, India

³Health Safety and Environment Group, BARC, Mumbai

ABSTRACT

The integrity assessment of the primary piping components needs to be demonstrated under normal operation cyclic loadings as well as under complex cyclic loadings of extreme magnitude as may come during a severe earthquake event. In order to understand material's cyclic plasticity and fatigue-ratcheting behaviour, systematic experimental and analytical investigations have been carried on specimens of SA333Gr.6 carbon steel and SS304LN stainless steel. The material specification of SA333Gr.6 is same as used in Primary Heat Transport (PHT) piping of Pressurized Heavy Water Reactors (PHWRs) and material specification of SS304LN steel is same as proposed for Indian Advance Heavy Water Reactor (AHWR's) Main Heat Transport (MHT) piping. The test program included the tensile, axial fatigue and uniaxial ratcheting tests to establish the material's mechanical properties and cyclic plasticity behavior. The results of these tests have been investigated in details using few popular finite element cyclic plasticity models to understand and quantify the material's cyclic plasticity behavior. The studies revealed the need to modify the Chaboche model to simulate the LCF/cyclic plasticity and ratcheting under different strain/stress amplitudes loading conditions. On accounting for modification, the Chaboche model nicely predicted the LCF and ratcheting response for all the tests. The tests, finite element analyses result and their interpretations have been presented in this paper.

Keywords: LCF, Ratcheting, Cyclic Softening/Hardening

1. INTRODUCTION

Mechanical Components of Nuclear Power Plant such as piping, vessels etc. are subjected to complex stresses/strains cyclic loading during the day to day operation loading and several other transients and events considered in designing of the components. In some situations, cyclic loading may induce large amplitude stress reversals, which exceed the elastic limit of the material and leads to Low Cycle Fatigue (LCF) damage. Under sustained (or primary) loading along with cyclic inelastic (or secondary) loading, in addition to LCF damage, progressive accumulation of deformation or strain (known as ratcheting) may also take place by ratchet action. Ratcheting is definition as the accumulation of plastic strain cycle-by-cycle for certain stress amplitude with a non-zero mean stress. The process of ratchet strain accumulation during cyclic loading causes reduction in the fatigue life of components and can lead to failure of components. Boussaa [1], Xia [2] etc. has shown significant influence of interaction on fatigue life of component. In view of this, safety and integrity of high energy pressurized piping system is of main concern and many researchers [3-4] have carried out experimental and analytical investigations. The investigations have shown that the fatigue-ratcheting synergy, leading to crack initiation and rupture in few cycles only, is the likely mode of failure [4]. In order to develop rational piping design methods for these failure

*Corresponding Author: Sumit Goyal, [Emailto:sgoyal@barc.gov.in](mailto:sgoyal@barc.gov.in), Ph: +912225591530, Fax: +912225505151

mechanisms, accurate prediction of ratcheting response is critical. In past, a number of investigators like Ohno et. al. [5], Chaboche et. al. [6], Bari et. al. [7] and Rahman et. al. [8] etc. has been carried out investigations to understand the cyclic plasticity and ratcheting behaviour of materials. Even though much research has been done on modeling of cyclic plasticity behaviour including ratcheting, none of the existing models in the literature is versatile and robust to simulate it accurately. Therefore, understanding and modeling of cyclic plasticity behavior still require several developments before robust plasticity models are constituted.

In view of it, systematic experimental and analytical investigations have been carried out to understand the cyclic plastic deformation and ratcheting behaviour of SA333Gr.6 carbon steel and SS304LN austenite stainless steel material. The test program included monotonic tensile, LCF and uniaxial ratcheting tests. The results of these tests have been investigated in details to understand and quantify the material's low cycle fatigue/cyclic plasticity and uniaxial ratcheting behaviour. Above specimen level investigations have generated data and helped in understanding the Indian PHWRs PHT and AHWRs MHT piping failure under complex cyclic loadings.

2. EXPERIMENTAL DETAILS AND RESULTS

Experiments are conducted on standard solid cylindrical specimens of SA333Gr.6 and SS304LN material. These specimens are fabricated in accordance with requirements of ASTM. In all, three types of uniaxial specimen tests have been conducted at room temperature (25°C to 30°C). It includes monotonic tensile test, Low Cycle Fatigue (LCF) test and uniaxial ratcheting tests.

2.1 Uniaxial Tensile Tests

Two numbers of monotonic tensile tests are carried out for each material to determine tensile properties at room temperature. Mechanical properties as evaluated from these tests are given in table 1.

2.2 Low Cycle Fatigue (LCF) Tests

LCF tests are conducted under strain controlled loading at different strain amplitudes ranging from 0.2 to 2.0%. These tests are performed under quasi-static cycling, in which strain rate was maintained at 0.001 (mm/mm)/sec. Table 2 gives the details of LCF tests, that is, specimen ID and applied strain amplitude in different tests. Data of these tests is used for evaluation of various cyclic plasticity model constants.

2.2.1 Cyclic Softening/Hardening Behavior

To evaluate the evolution of stress-strain response with number of cycles, that is, cyclic softening/ hardening behaviour of material, test data of LCF have been analyzed in detail. It is observed that the stress-strain response of both materials changes cycle-by-cycle, until it gets stabilized in few cycles. Typical stress amplitude variations with number of cycles, for 1.0% & 2.0% strain amplitude of SS304LN material is shown in fig. 1(a & b). From these figures, it is observed that SS304LN material show cyclic hardening in initial few cycles, which is termed as primary cyclic hardening. The stress amplitude variation is still observed until failure, however the rate of change is insignificantly small in comparison to that during initial cycles and it is termed as secondary cyclic softening/hardening. For SS304LN primary cyclic hardening is followed by cyclic softening or cyclic hardening depending upon the strain amplitude. On the other hand, SA333Gr.6 material shows primary cyclic softening/hardening depends on applied strain amplitude followed by secondary cyclic hardening. The variation of stress amplitude response versus strain amplitude for SA333Gr.6

has been plotted with different number of cycles in fig. 1(c). These iso-cycle curves clearly show that the stress amplitude response is not only function of number of cycles (N) but also depends on applied strain amplitude.

2.2.2 Evaluation of Stabilized or Cyclic Stress-Strain Curve

In view of cyclic softening/hardening behavior, material's cyclic stress-strain curve is evaluated using half life criterion in the present work. Value of stabilized stress amplitude is acquired from the stable hysteresis loop corresponding to the applied strain amplitude in the different LCF tests. Stable hysteresis loops for different given strain amplitudes and corresponding saturated stress amplitude is shown in fig. 2 and table 2 respectively. Final cyclic stress-strain curve is idealized by Ramberg-Osgood (R-O) equation, as given in Eq. (1) below:

$$\frac{\Delta\varepsilon}{2} = \frac{\Delta\sigma}{2E} + \frac{1}{2} \left\{ 2 \left(\frac{\Delta\sigma}{2} \right) \frac{1}{K} \right\}^{\left(\frac{1}{n} \right)} \quad (1)$$

The constants of Eq. (1) are evaluated by fitting the cyclic stress-strain data ($\Delta\sigma/2$, $\Delta\varepsilon/2$). The value of R-O constants (k & n) is 1612.5 & 0.18 for SA333Gr.6 and 5714.6 & 0.47 for SS304LN. Comparison of stabilized stress-strain data and R-O fitted curve with monotonic stress-strain curve is shown in fig. 2.

3 FINITE ELEMENT SIMULATION OF CYCLIC PLASTICITY BEHAVIOUR

The fatigue design of components/structures depends on the precise evaluation of local strains, during their finite element analyses etc. Hence, the fatigue tests results is further investigated to establish a robust cyclic plasticity model for the material under consideration. Chaboche's [6], nonlinear kinematic hardening model is one of the widely accepted cyclic plasticity models. Chaboche three decomposed model has been used and its parameters have been evaluated using LCF tests data.

3.1 Determination of Chaboche Model Parameter and Its Performance

Chaboche three-decomposed model uses Von-Mises yielding criterion and associated incremental plasticity flow rule as given below:

$$f(\sigma_{ij}, \alpha_{ij}) = \sqrt{\frac{3}{2} (\tau_{ij} - a_{ij})(\tau_{ij} - a_{ij})} - \sigma_o = 0 \quad \text{and} \quad d\varepsilon_{ij}^p = \lambda \frac{\partial f}{\partial \sigma_{ij}} \quad (2)$$

In the above equations, σ_{ij} is the stress tensor, α_{ij} is the total backstress tensor, τ_{ij} is the deviatoric part of σ_{ij} , a_{ij} is the deviatoric backstress tensor, σ_o is the size of yield surface, ε_{ij}^p is the plastic strain tensor, $d\varepsilon_{ij}^p$ is increment in ε_{ij}^p , and λ is a positive scale factor of proportionality. Total stress at any point in uniaxial stress-strain hysteresis loop, is the sum of σ_o and α_x . Total backstress can be represented as the summation of three backstress components due to each of the kinematic hardening rule.

$$\sigma_x = \alpha_x + \sigma_o \quad \text{and} \quad \alpha_x = \sum_{i=1}^3 \alpha_i = \alpha_1 + \alpha_2 + \alpha_3 \quad (3)$$

Chaboche proposed that the increment of backstress in deviator stress space can be defined as (where p is the accumulated plastic strain):

$$da = \sum_{i=1}^M da_i \quad \text{and} \quad da_i = \frac{2}{3} C_i d\varepsilon^p - \gamma_i a_i dp \quad (4)$$

Chaboche three decomposed model have total seven parameters, namely, σ_o , C_1 , γ_1 , C_2 , γ_2 , C_3 and γ_3 . Out of these, six parameters are evaluated from stable σ - ε hysteresis loop of LCF test. The value of γ_3 , ratcheting parameter, needs to be evaluated using uniaxial ratcheting data.

Chaboche model parameters for SA333Gr.6 and SS304LN have been evaluated using stable hysteresis loop of $\pm 0.85\%$ and $\pm 1.0\%$ strain amplitude LCF test, respectively. The value of σ_o is taken to be equal to cyclic yield stress which in present work is evaluated from stable hysteresis loop corresponding to the half of the linear portion by 0.02% strain offset. It has been seen that up to 0.02% offset strain the effect of non-linearity is insignificant, therefore σ_o definition is subjective and based on judgment. Comparison of FE simulated stable hysteresis loop (using evaluated model parameters) with test is shown in fig. 3(a) and fig. 4(a), for 0.85% strain amplitude of SA333Gr.6 and 1.0% strain amplitude of SS304LN, respectively. It is evident from the comparison that predicted hysteresis loop is very closely matches with respect to test results.

Same set of parameters is used for the FE simulation of other axial fatigue tests, in order to verify the applicability of evaluated Chaboche model parameters. The comparisons of simulated stable hysteresis loops for strain amplitude 0.7%, 1.0% and 1.4% with corresponding tests result are shown in fig. 3(b) and fig. 4(b) for the two materials. It is observed from the figure that for strain amplitude 0.7% and for 1.4%, it over and under predicts the stress-strain hysteresis loop, respectively. The stress amplitude response as evaluated by FE analyses are also compared against those which are recorded in tests for each of applied strain amplitude, shown in fig. 3(c) and fig. 4(c). It is observed from this figure that evaluated stress amplitude is deviates from the corresponding stress amplitude as recorded in the test. The possible cause for this deviation is elaborated in next subsection.

3.2 Evolution of Size of Yield Surface (σ_o) and C_3 Parameter

In view of above discussion, hysteresis loops for different LCF tests are compared, as shown in fig. 5. For this comparison, loops are rigidly shifted in stress-plastic strain plane such that departure from linearity (or starting point of non-linearly, corresponds to 0.02% offset) of all loops could match. From the comparison, it is clear SA333Gr.6 shows masing behavior except linear portion, represents twice of σ_o , which shows dependence on applied strain. However, SS304LN shows non-masing behavior. Thus, single set of Chaboche model parameters can not model all the loops for non-masing materials. It is concluded that there is requirement of different value of parameters for simulation of different loops depending on the applied strain amplitudes. This observation has not been considered in widely used cyclic plasticity models. Based on LCF experimental data, value of σ_o and C_3 are determined for each test directly from the corresponding stable hysteresis stress-strain loop and can be best represented as a function of plastic strain amplitude ($\Delta\varepsilon_p/2$) as given below:

$$\text{SA333Gr.6 : } \sigma_o = 133.86e^{0.4074(\Delta\varepsilon_p/2)} \text{ MPa} \quad \text{and} \quad C_3 = 4150 \text{ Mpa}$$

$$\text{SS304LN : } \sigma_o = 137.396e^{0.3616(\Delta\varepsilon_p/2)} \text{ MPa} \quad \text{and} \quad C_3 = 1863.6 \left[1 + \left(\frac{\Delta\varepsilon_p}{2} \right)^{-1.4233} \right] \text{ MPa}$$

3.3 Modification in Chaboche Three Decomposed Model

It is clear that for the simulation of hysteresis loops of different strain amplitude for SS304LN, non-masing material, there is requirement of evaluation of individual set of Chaboche model parameters. However, for SA333Gr.6, masing material, same set of rest parameters will work. In view of this, experimental σ - ε hysteresis loops of SS304LN have been reanalyzed in detail. Parameters (C_1, γ_1) represent the first region of hysteresis loop, that is, onset of non-linearity, therefore, these can be taken as constant for all the hysteresis loops under consideration. Now value of other two parameters (C_2, γ_2) is evaluate from different

stable hysteresis loops and can be best represent as a function of plastic strain amplitude ($\Delta\epsilon_p/2$) as given below:

$$\text{SS304LN : } C_2 = 77000 \left[1 - e^{-3.1(\Delta\epsilon_p/2)} \right] \text{ MPa and } \gamma_2 = 169.44 \left[1 + \left(\frac{\Delta\epsilon_p}{2} \right)^{-0.823} \right]$$

The stable hysteresis loops of different strain amplitude are simulated again by FE analysis using Chaboche parameters as function of strain amplitude. The FE results are compared with experimental results, as shown in fig. 6. It is observed that by considering dependence of parameters on strain amplitude, the comparison with experimental results is nearly perfect. In this case, the peak stress response is exactly simulates (for different strain amplitudes) unlike the case in which all chaboche parameters are treated as constant, see fig. 4 and fig. 6. Finally, it is clear from the above analysis that Chaboche model with proposed modifications, that is, dependence of model parameters on strain amplitude, is able to simulate the stable LCF response satisfactorily for all the different loading ranges considered.

3.4 Uniaxial Ratcheting Tests and Simulation using Chaboche Model

Uniaxial ratcheting tests are conducted under stress controlled loading under various combinations of mean stress (M) and stress amplitude (A). For SA333Gr.6 values of M & A stresses are (40, 80, 120) MPa & (270, 310, 350) MPa and for SS304LN it is (60, 120, 180) MPa & (300, 360, 420) MPa is considered. From the analysis of strain history of these tests, ratcheting strain as well as strain range variation with cycle is evaluated. Ratcheting strain is taken to be the maximum values of strain in a cycle and strain range is taken as the difference of maximum and minimum strain. Experimental results show that accumulation of ratchet strain increases with increase in mean stress and/or stress amplitude.

Test data of these tests is used for the evaluation of seventh parameter of Chaboche model γ_3 , ratcheting parameter. As discussed earlier that cyclic yield stress strongly depends on the strain amplitude/range. Therefore value of cyclic yield stress is evaluated on the basis of strain range prediction, as observed in actual test. For FE analysis other Chaboche model parameters are used corresponding to the stable strain amplitude in the test. In the present analysis of these tests, FE simulation is performed for initial 100 cycles only. First of all, simulation of M80A310 is carried out with different values of γ_3 (1, 1.5, 2.0, and 2.5) and compared with experiment in fig. 7(a). From the figure, it is clear that absolute values of ratchet strain accumulation are not matching in any of these cases. It may be noted that carbon-manganese shows Luders bands (see monotonic stress-strain curve in fig. 2b) and due to it, the basic stress strain curve is discontinuous. Further, due to cyclic softening in this region of strain range, which takes place in initial few cycles before stabilization, actual accumulation will be more. In view of these, to account the difference in strain due to Luders band and cyclic softening effect before stabilization, a constant shift was applied and predicted strain accumulations are re-plotted in fig. 7(b). From this figure, it is clear that out of various values, γ_3 equal to 2 shows closer match with experiment. Figure 7(c) plot the FE results with experiments for a set (constant Mean stress with different Mean stress amplitude) of SA333Gr.6. It shows that rate of ratcheting is well simulated for most of the cases. Similarly value of parameter γ_3 is also evaluated for SS304LN material which is found equal to 1.5.

From the analysis, it is observed that Chaboche model with proposed modifications is able to simulate ratcheting rate only. It is also clear that overall prediction in ratcheting response is satisfactory but still not accurate in all the regimes. This is due to cyclic softening/hardening

of the material before stabilization. Further development in cyclic plasticity models is essential to account phenomena such as cyclic hardening/softening.

4. CONCLUSION

The Experimental and analytical investigations have been carried out to understand cyclic plasticity response of SA333Gr.6 and SS304LN materials. The insights gained from the tests followed FE analysis are discussed here:

- SS304LN material show cyclic hardening in initial few cycles, which is termed as primary cyclic hardening followed by cyclic softening or cyclic hardening, termed as secondary, depending upon the strain amplitude until failure. SA333Gr.6 shows strain amplitude dependent primary cyclic softening/hardening followed by secondary cyclic hardening.
- Material showed non massing behavior therefore, single set of 3-decomposed Chaboche model parameters are unable to simulate cyclic plastic (LCF) response for different strain ranges. For SA333Gr.6 size of cyclic yield surface (σ_0) and for SS304LN σ_0 along with three-decomposed Chaboche model parameters like C_2 , γ_2 and C_3 are found to be strong function of strain range.
- To simulate LCF response for different strain ranges, the dependence of yield surface (σ_0), C_2 , γ_2 and C_3 on strain range must be accounted. Classical Chaboche model does not account it, since these parameters are assumed as material constants. In current paper, a modification to Chaboche model is proposed where these parameters are taken as function of strain range. The modified model very closely simulated the cyclic plastic (LCF) response for all the LCF tests under consideration. Although it's general numerical implementation needs to be developed.
- Chaboche model with proposed modifications is able to simulate uniaxial ratcheting rate only. This is due to cyclic hardening of the material before stabilization, which is not considered in Chaboche model.

Further development in cyclic plasticity models is essential to account phenomena such as cyclic hardening/softening, extra hardening due to multiaxial and non-proportional loading.

REFERENCES

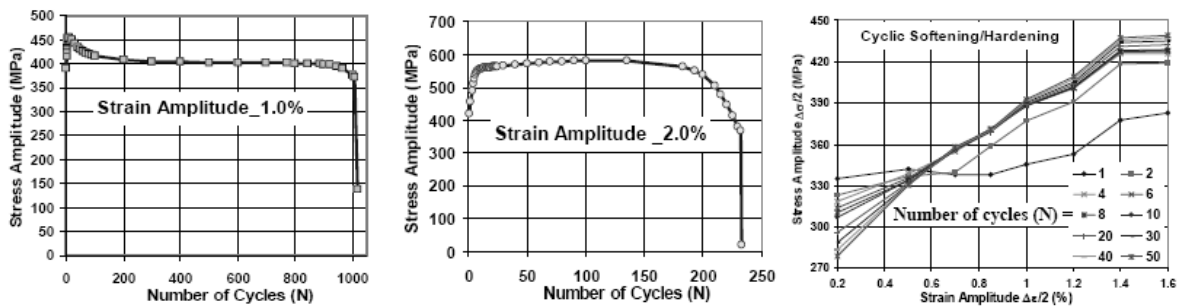
- [1] Boussaa D., Van, K.D., Labbe, P., Tang, H.T., "Fatigue–Seismic Ratcheting Interactions in pressurized Elbows", *Journal of Pressure Vessel Technology*, Vol. 116, 1994, pp. 396-402.
- [2] Xia, Z., Kujawski, D. and Ellyin, F., "Effect of mean stress and ratcheting strain on fatigue life of steel", *International Journal of Fatigue*, Vol. 18, 1996, pp. 335-341.
- [3] Touble, F., Baly, N. and Lacire, M. H., "Experimental, Analytical and regulatory evaluation of seismic behaviour of piping system", *ASME Journal of Pressure Vessel Technology*, Vol. 121, 1999 pp. 388-392.
- [4] Suneel K. Gupta, Sumit Goyal, Vivek Bhasin, Vaze K.K., Ghosh A.K, Kushwaha H.S., "Ratcheting-Fatigue Failure of Pressurized Elbows made of Carbon Steel", *SMiRT-20*, Finland, 2009
- [5] Ohno, N., Kachi, Y., "A constitutive model of cyclic plasticity for nonlinear hardening materials" *Journal of Appl. Mech.*, Vol. 53, 1986, pp. 395–403.
- [6] Chaboche, J. L., "On some modifications of kinematic hardening to improve the description of ratcheting effects", *International Journal of Plasticity*, Vol. 7, 1991, pp. 661–678.
- [7] SHAFIQU, BARI, "Constitutive Modeling for Cyclic Plasticity and Ratcheting", *Ph.D Thesis*, North Carolina State University, 2001.
- [8] Rahman, S. M., Hassan, T., Edmundo, C., "Evaluation of cyclic plasticity models in ratcheting simulation of straight pipes under cyclic bending and steady internal pressure", *International Journal of Plasticity*, Vol. 24, 2008, pp. 1756–1791.

Table 1: Mechanical Properties of materials

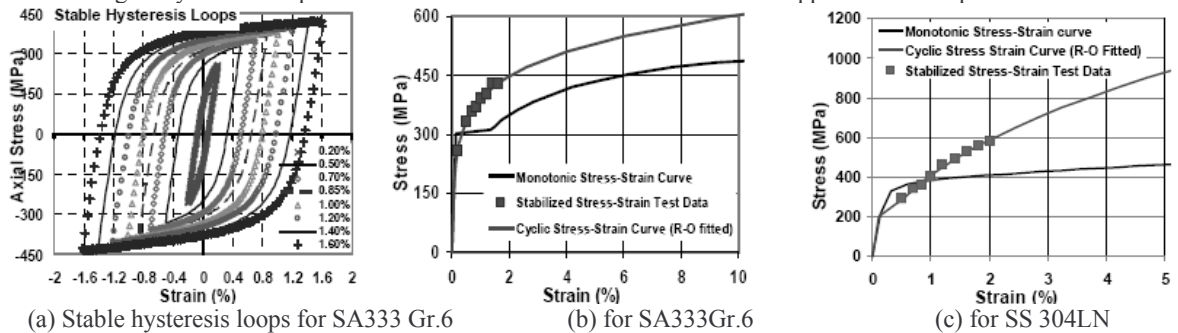
Properties	Yield Stress σ_y (MPa)	Ultimate Stress σ_u (MPa)	Elongation (%)	Young's Modulus E (GPa)
SA333 Gr.6	304	500	28	203
SS304LN	340	670	65	195

Table 2: Details of LCF tests

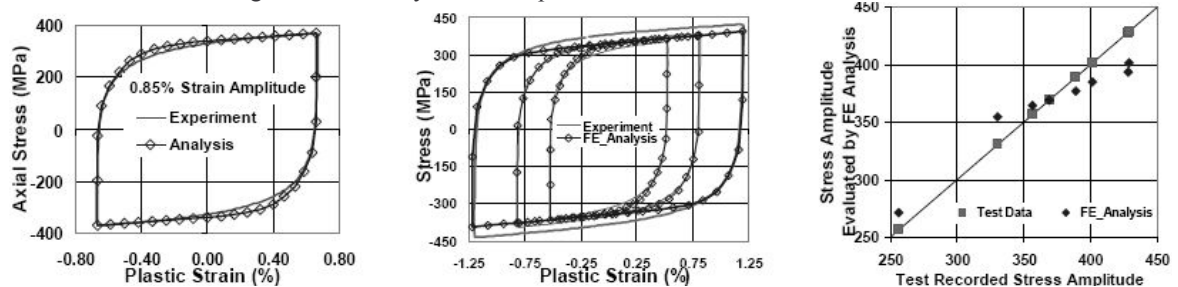
Specimen ID	LCF1	LCF2	LCF3	LCF4	LCF5	LCF6	LCF7	LCF8	LCF9	LCF10	
Strain Amplitude (%)	0.2	0.5	0.7	0.85	1.0	1.2	1.4	1.6	1.8	2.0	
Saturated Stress Amplitude (MPa)	SA333 Gr.6	257	331	356	369	389	402	428	429	---	---
	SS304LN	---	290	342	361	402	459	497	530	560	582



(a) σ Vs N (ϵ , 1.0%), SS304LN (b) σ Vs N (ϵ , 2.0%), SS304LN (c) Cyclic softening/hardening, SA333Gr.6
 Fig. 1 Cyclic σ - ϵ responses of SS304LN and SA333Gr.6 at different applied strain amplitude.



(a) Stable hysteresis loops for SA333 Gr.6 (b) for SA333Gr.6 (c) for SS 304LN
 Fig. 2 Stabilized hysteresis loops and stabilized stress-strain curve.



(a) σ Vs ϵ_p for (ϵ , 1.0%) (b) σ Vs ϵ_p for (ϵ , 0.7%, 1.0% & 1.4%) (c) Peak stress comparison
 Fig. 3 Comparison of stable σ - ϵ response for various strain amplitude of SA333Gr.6 using single set of Chaboche parameters

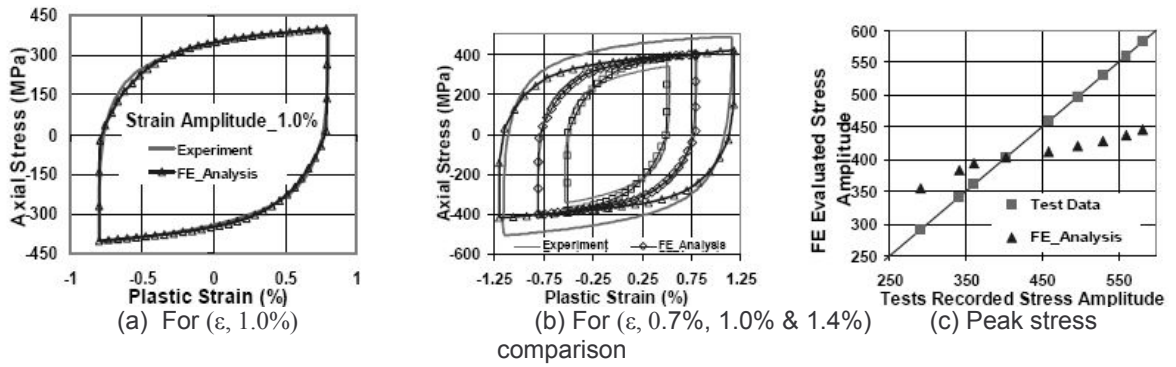


Fig. 4 Comparison of stable σ - ϵ response for various strain amplitude of SS304LN using single set of Chaboche parameters

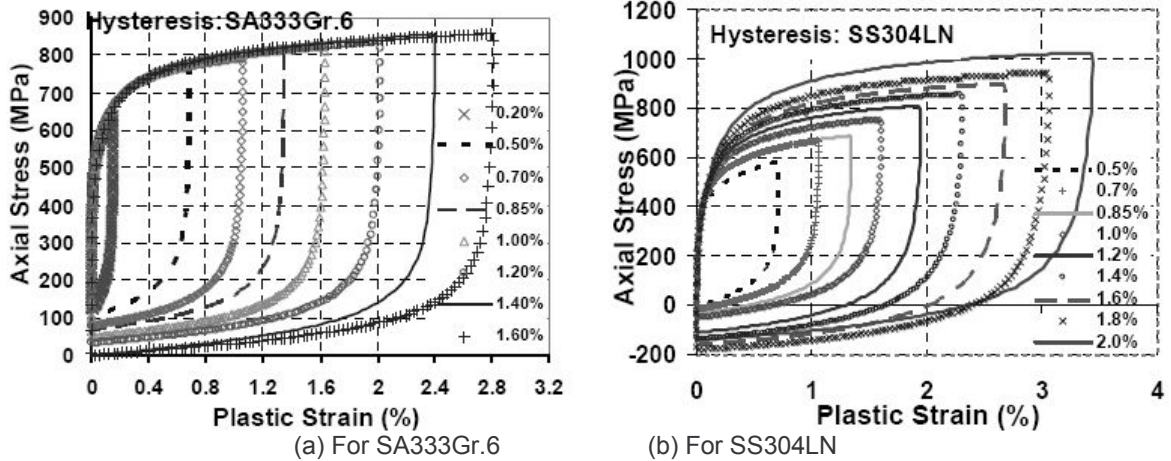


Fig. 5 Comparison of liner portion in hysteresis loops of different strain amplitudes

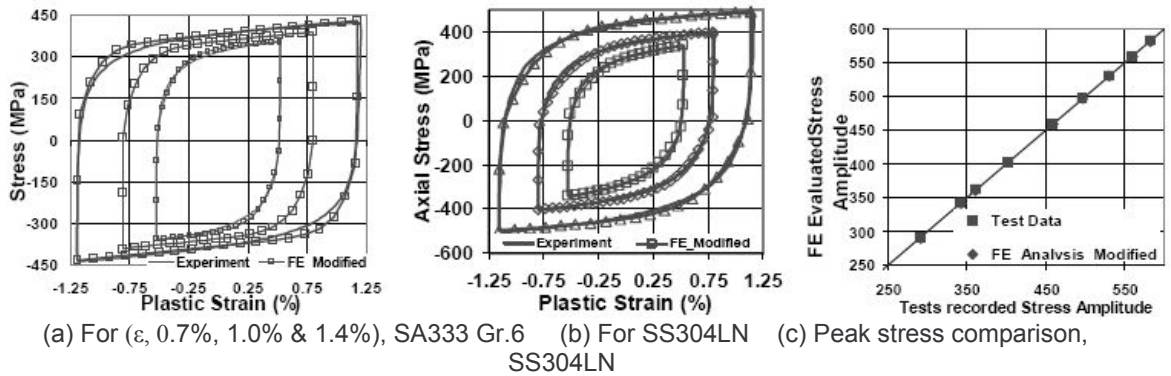


Fig. 6 Comparison of stable σ - ϵ response for various strain amplitude using Chaboche model (Using individual/different set of parameter)

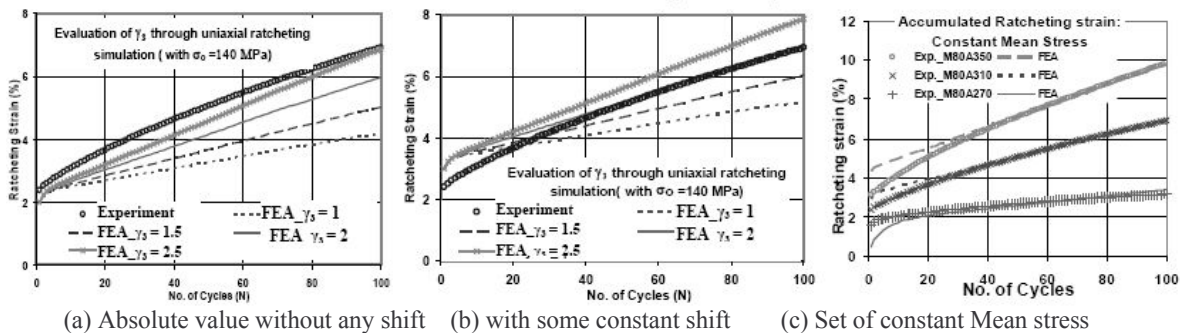


Fig. 7 Comparison of ratcheting strain response of FE analyses with experiments for SA333Gr.6 material.